Theoretical Study on Structures and Aromaticities of P_5^- Anion, [Ti (η^5-P_5)]$^-$ and Sandwich Complex [Ti(η^5-P_5)$_2$]$^{2-}$

Zi-Zhong Liu,[†,§,||] Wei-Quan Tian,[‡] Ji-Kang Feng,*[,†,§] Gang Zhang,[†] and Wei-Qi Li[†]

State Key Laboratory of Theoretical and Computational Chemistry, Institute of Theoretical Chemistry, JiLin University, Chang Chun 130023, China, Department of Chemistry, University of British Columbia, 2036 Main Mall, Vancouver, British Columbia V6T 1Z1, Canada, The College of Chemistry, JiLin University, Chang Chun 130023, China, and Chemistry and Environment Science College, Inner Mongolia Normal University, Huherhort, 010022 China

Received: December 9, 2004; In Final Form: March 27, 2005

The equilibrium geometries, energies, harmonic vibrational frequencies, and nucleus independent chemical shifts (NICSs) of the ground state of P_5^- (D_{5h}) anion, the [Ti (η^5-P_5)]$^-$ fragment (C_{5v}), and the sandwich complex [Ti(η^5-P_5)$_2$]$^{2-}$ (D_{5h} and D_{5d}) are calculated by the three-parameter fit of the exchange-correlation potential suggested by Becke in conjunction with the LYP exchange potential (B3LYP) with basis sets 6-311+G(2d) (for P) and 6-311+G(2df) (for Ti). In each of the three molecules, the P−P and Ti−P bond distances are perfectly equal: five P atoms in block P_5^- lie in the same plane; the P−P bond distance increases and the Ti−P bond distance decreases with the order P_5^-, [Ti(η^5-P_5)$_2$]$^{2-}$, and [Ti (η^5-P_5)]$^-$. The binding energy analysis, which is carried out according to the energy change of hypothetic reactions of the three species, predicts that the three species are all very stable, and [Ti (η^5-P_5)]$^-$ (C_{5v}), more stable than P_5^- and [Ti(η^5-P_5)$_2$]$^{2-}$ synthesized in the experiment, could be synthesized. NICS values, computed for the anion and moiety of the three species with GIAO−B3LYP, reveal that the three species all have a larger aromaticity, and NICS (0) of moiety, NICS (1) of moiety, and minimum NICS of the inner side of ring P_5 plane in magnitude increase with the order P_5^-, [Ti(η^5-P_5)$_2$]$^{2-}$, and [Ti (η^5-P_5)]$^-$. By analysis of the binding energetic and the molecular orbital (MO) and qualitative MO correlation diagram, and the dissection of total NICS, dissected as NICS contributions of various bonds, it is the main reason for P_5^- (D_{5h}) having the larger aromaticity that the P−P σ bonds, and π bonds have the larger diatropic ring currents in which NICS contribution are negative, especially the P−P σ bond. However, in [Ti (η^5-P_5)]$^-$ (C_{5v}) and [Ti(η^5-P_5)$_2$]$^{2-}$ (D_{5h}, and D_{5d}), the reason is the larger and more negative diatropic ring currents in which the NICS contributions of P−P π bonds and P_5−Ti bonds including π, δ, and σ bonds, especially P_5−Ti bonds, are much more negative and canceled the NICS contributions of P and Ti core and lone pair electrons.

I. Introduction

Aromaticity, a fundamental chemical concept, emerged with the isolation of benzene due to its aroma in 1825[1]. The terms "aromatic" and "aromaticity" are used to described cyclic, planar, and conjugated molecules with $4n + 2$ π electrons and special chemical and structural stability. Despite the broad application of aromaticity, it has been only applied to the domain of conjugated organic compounds. Based on experimental and theoretical evidence of aromaticity in an all-metallic Al_4^{2-} dianion in a series of bimetallic ionic system with chemical composition MAl_4^- (M = Li, Na, or Cu),[2,3] aromaticity and antiaromaticicity were extended to the regime of all-metal clusters,[4−7] which have highly magnetic properties, large ring currents, similar derived aromatic structures, and large resonance energies, and then they are further extended to inorganic field, such as the system of polyphosphaphospholes,[8] of pentaphosphaferrocene,[9] and of others.[10−25] Especially, the concept of multiplefold aromaticity, present in molecules that possess more than one independent delocalized bonding system, either σ-type or π-type, was also applied to sandwich-like complexes on "all-metal (Al_4^{2-})" aromatic compounds.[9(b)] This new concept should help one to understand the simultaneous contributions to aromaticity within the same molecular structures arising from various delocalized bonding systems of the molecule. New aromatic compounds have recently been identified whose incorporation into sandwich complexes opens new routes for chemical creativity.[9(c)] Schleyer et al. proposed nucleus-independent chemical shifts (NICS) as a simple and efficient aromaticity probe,[26] which is applied to both organic and inorganic compounds.[27] Negative NICSs denote aromaticity, positive NICSs denote antiaromaticity, and zero NICS means nonaromaticity. The magnitude of NICSs indicates the degree of aromaticitiy or antiaromaticity.[26] This new broadly applied concept of NICS helps one to understand the contributions to aromaticity within the same molecule arising from various delocalized bonding systems of molecules.

Since the first synthesis of pentamethylpentaphosphaferrocene by Scherer and co-workers,[28] and pentaphosphacyclopentadienide, the P_5^- anion, by Baudler and co−workers,[29] the structure

* To whom correspondence should be addressed.
† Institute of Theoretical Chemistry, JiLin University.
‡ University of British Columbia.
§ The College of Chemistry, JiLin University.
|| Inner Mongolia Normal University.

10.1021/jp044395a CCC: $30.25
Published on Web 06/08/2005

and synthesis of pentaphosphametallocene and the aromaticity of polyphosphaphospholes and the P_5^- anion have attracted much attention from the chemical community by the fact that metallocene and analogous organometallic compounds have found many applications as synthetic reagents, catalysts of polymerization and hydrogenation of olefin, and building blocks for new materials (e.g., polyferrocenes).[8(e),30,31] Recently, Schleyer and co-workers[32] studied reactions of highly reduced titanium complexes with white phosphorus and found that at or below 25 °C the reactions yield brown to deep red-brown salts of inorganic metallocene $[K(18\text{-Crown-6})]_2[Ti(\eta^5-P_5)_2]$. Like ferrocenes and other carbon-based metallocenes, $[Ti(\eta^5-P_5)_2]^{2-}$ has parallel and planar five-membered rings symmetrically positioned beside the central metal atom. Despite its electron-deficient and formally zerovalent character of titanium, the salts are highly stable toward heat and air both in solution and in the solid state.[32] The structure and bonding of the sandwich complexes $[Ti(\eta^5-E_5)_2]^{2-}$ (E = CH, N, P, As, Sb) were theoretically reported by Lein and co-workers.[33] However, no aromaticity of this compound and nature of the metal−ligand interaction has been studied. The detailed studies on aromaticity and electronic structure of $[Ti(\eta^5-P_5)_2]^{2-}$ can help to understand the unusual stability of $[Ti(\eta^5-P_5)_2]^{2-}$ salt and reveal the nature of bonding between Ti and P_5^-.

II. Computational Methods

The geometries were first optimized, and frequencies of P_5^-, $[Ti\ (\eta^5-P_5)]^-$, and $[Ti\ (\eta^5-P_5)_2]^{2-}$ were calculated by DFT/B3LYP and Hartree-Fock (HF) methods with 6-311+G(2d) for P and 6-311+G(2df) for Ti. More extended 6-311+G(3df,3pd) with polarized split-valence basis sets (6−311++G(d, p)) are used. The two most stable structures for $[Ti(\eta^5-P_5)_2]^{2-}$, the eclipsed configuration (D_{5h}) and the staggered configuration (D_{5d}), the most stable structure for $[Ti\ (\eta^5-P_5)]^-$ (C_{5v}) and for P_5^- (D_{5h}), were found. All of the stationary points were verified with vibrational frequency calculations in which Hessians (the second-order derivative of total energy with respect to nuclear coordinates on the potential energy surface (PES)) were calculated. If all of the eigenvalues in the Hessian are positive for a stationary point, this stationary point is a minimum on PES. One or more negative eigenvalues of a stationary point indicates the saddle point nature of this stationary point on the PES. The NICSs of every structure in different positions were predicted with DFT/B3LYP and Hartree−Fock (HF) methods with the same basis sets as employed in geometry optimization. All calculations were performed with the Gaussian 03 program.[34] Molecular wave function were calculated at the DFT/B3LYP/6-311++G(d, p) level of theory, and MOs were plotted with the MOLDEN 3.9 program.[35]

III. Results and Discussion

The optimized geometric structures for the P_5^- anion, $[Ti\ (\eta^5-P_5)]^-$, and $[Ti\ (\eta^5-P_5)_2]^{2-}$ are shown in Figure 1. [Ti (η^5−

TABLE 1: Bond Distances (Angstrom), Relative Energies (a u), and the Number of Imaginary Frequencies (NIF) at the B3LYP/gen Level for P_5^-, $[Ti\ (\eta^5\text{-}P_5)_2]^{2-}$, and $[Ti\ (\eta^5\text{-}P_5)]^-$

species	sym	r(P−P)(Å)	r(Ti−P) (Å)	E(a.u.)	NIF
P_5^-	D_{5h}	2.120		2556.511	0
$[Ti\ (P_5)_2]^{2-}$	D_{5h}	2.175	2.606	0.000	0
$[Ti\ (P_5)_2]^{2-}$	D_{5d}	2.169	2.621	0.009	1
$[Ti\ (P_5)_2]^{2-a}$	C_1	2.1689∼2.1690	2.6207∼2.6208	0.00898	1
$[Ti\ [P_5)]^-$	C_{5v}	2.240	2.382	1707.049	0

[a] Maximum of distorted bond angle $\Delta\alpha \leq 0.005°$, maximum of distorted dihedral angel $\Delta\beta \leq 0.004°$.

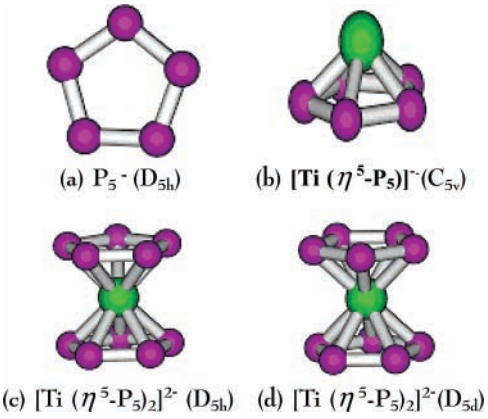

Figure 1. Molecular structure.

TABLE 2: Binding Energies for P_5^-, $[Ti\ (\eta^5\text{-}P_5)_2]^{2-}$, and $[Ti\ (\eta^5\text{-}P_5)]^-$ According to the Imaginary Reaction (kcal/mol) at the B3LYP/gen Level

species	sym	ΔE_1	ΔE_2	ΔE_3	ΔE_4	ΔE_5
P_5^-	D_{5h}		397.5			
$[Ti\ (P_5)_2]^{2-}$	D_{5h}	118.0	913.1	199.1	81.1	10.2
$[Ti\ (P_5)_2]^{2-}$	D_{5d}	112.3	907.4	189.5	77.1	4.6
$[Ti\ (P_5)]^-$	C_{5v}	107.8	505.3	119.6		

$P_5)_2]^{2-}$ has an eclipsed form (with D_{5h} symmetry) and a staggered form (with D_{5d} symmetry). Computed results, calculated bonding distances, total energies, and the number of imaginary frequencies of all conformations with the B3LYP/gen (P:6-311+G(2d),Ti:6-311+G(2df)) method are listed in Table 1. The calculated binding energies of proposed reactions 1−5, 1′, 2′, and 2″ for the three molecules at the B3LYP/gen level are listed in Table 2.

$$[Ti\ (\eta^5-P_5)_2]^{2-}\ (^1A_1, D_{5h}) \rightarrow 2\ P_5^-\ (^1A_1, D_{5h}) + Ti\ (^1G)\ \Delta E_1 \quad (1)$$

$$[Ti\ (\eta^5-P_5)]^-\ (^1A_1, C_{5v}) \rightarrow P_5^-\ (^1A_1, D_{5h}) + Ti\ (^1G)\ \Delta E_1 \quad (1')$$

$$[Ti\ (\eta^5-P_5)_2]^{2-}\ (^1A_1, D_{5h}) \rightarrow 8\ P\ (^4S) + 2P^-\ (^1D) + Ti\ (^1G)\ \Delta E_2 \quad (2)$$

$$[Ti\ (\eta^5-P_5)]^-\ (^1A_1, C_{5v}) \rightarrow 4\ P\ (^4S) + P^-\ (^1D) + Ti\ (^1G)\ \Delta E_2' \quad (2')$$

$$P_5^-\ (^1A_1, D_{5h}) \rightarrow 4\ P\ (^4S) + P^-\ (^1D)\ \Delta E_2'' \quad (2'')$$

$$[Ti\ (\eta^5-P_5)_2]^{2-}\ (^1A_1, D_{5h}) \rightarrow [(\eta^5-P_5)-(\eta^5-P_5)]^{2-}\ (^1A_1, D_{5h}) + Ti\ (^1G)\ \Delta E_3 \quad (3)$$

$$2\ P_5^-\ (^1A_1, D_{5h}) \rightarrow [(\eta^5-P_5)-(\eta^5-P_5)]^{2-}\ (^1A_1, D_{5h})\ \Delta E_4 \quad (4)$$

$$[Ti\ (\eta^5-P_5)_2]^{2-}(^1A_1, D_{5h}) \rightarrow [Ti\ (\eta^5-P_5)]^-\ (^1A_1, C_{5v}) + P_5^-\ (^1A_1, D_{5h})\ \Delta E_5 \quad (5)$$

NICS values were computed at 0.25 Å successions of points above and beneath the ring center using B3LYP/gen (P: 6-311+G(2d), Ti: 6-311+G(2df) level. The calculated NICSs of the optimized structures, at the ring center, 1 Å above the ring center, and minimum NICS beneath the ring center, were listed in Table 3. The same results with the other four methods are shown in the Supporting Information.

A. Structure and Stability. Our studies on P_5^- (D_{5h}), $[Ti\ (\eta^5-P_5)]^-$ (C_{5v}), and $[Ti\ (\eta^5-P_5)_2]^{2-}$ (D_{5h} and D_{5d}) indicate that

TABLE 3: Total Nucleus Independent Chemical Shift (NICS) Values for P_5^-, [Ti (η^5-P_5)$_2$]$^{2-}$, and [Ti (η^5-P_5)]$^-$(ppm) at the B3LYP/gen Level

species	sym		NICS(0)	NICS(1)
P_5^-	D_{5h}		−15.4	−14.8
				(−15.7)[c]
[Ti (P_5)$_2$]$^{2-}$	D_{5h}	*a*	−36.8	−21.1
		b		−45.8
[Ti (P_5)$_2$]$^{2-}$	D_{5d}	*a*	−37.8	−21.5
		b		−50.6
[Ti (P_5)]$^-$	C_{5v}	*a*	−73.1	−34.4
		b		−78.1

[a] Outer plane $r = 1$ Å. [b] The most negative NICS in inner plane, $r = 0.50$ Å (P_5^-), $r = 0.75$ Å ([Ti (η^5−P_5)$_2$]$^{2-}$), $r = 0.25$ Å ([Ti (η^5−P_5)]$^-$). [c] The most negative NICS outer plane, $r = 0.50$ Å (P_5^-).

all P−P bond distances in P_5^-, [Ti (η^5−P_5)]$^-$ (C_{5v}), and [Ti (η^5−P_5)$_2$]$^{2-}$ (D_{5h} or D_{5d})) are equal, intermediate between P−P single bond distance (2.21 Å) and P═P double bond distance (2.02 Å),[32] and that all Ti−P bond distance in [Ti (η^5−P_5)]$^-$ (C_{5v}) or [Ti (η^5−P_5)$_2$]$^{2-}$ (D_{5h} and D_{5d}) are equal. These results are in agreement with previous studies.[8,32,33]

We found that, in gas and no [K(18-Crown-6)] in (P_5)$_2$Ti, the D_{5h} form is the ground-state, and is 5.6 kcal/mol lower in energy at B3LYP/gen level than C_1 form which has a imaginary frequency in the Hessian calculation, in which all of the P−P bond distances are not equal, too, from 2.1689 to 2.1690 Å, so are P−Ti bond distances, from 2.6207 to 2.6208 Å. But, in the crystal structure and in the state in which there are [K(18-Crown-6)] in (P_5)$_2$Ti, because the interaction between atoms and bases and John Teller distortion induce the D_{5h} form to distort the C_1 form, it makes the C_1 form becoming the ground-state in which all of P−P bond distances are not equal in the experiment,[32] extent from 2.1469 to 2.1608 Å, P−Ti bond distances extent from 2.5443 to 2.5811 Å.

On the basis of the binding energies by hypothetical reactions 2, 2′, and 2″, which are used to calculate binding energies between all of the atoms, the values of the binding energies (ΔE_2) for P_5^- (D_{5h}), the fragment [Ti (η^5−P_5)]$^-$ (C_{5v}), and [Ti (η^5−P_5)$_2$]$^{2-}$ (D_{5h}) are all very big. It indicates that three species are so stable that this result is in agreement with the fact that P_5^- (D_{5h}) and [Ti (η^5−P_5)$_2$]$^{2-}$ (C_1) had been synthesized in experiment and that [Ti (η^5−P_5)]$^-$ (C_{5v}) can be synthesized.

Based on reaction 5, we calculated the first dissociation energy of the P_5^-−Ti−P_5^- bond (ΔE_5), which is only 10.2 kcal/mol (D_{5h}) at the B3LYP/gen. However, Ti−P_5^- dissociation energies, which is the second dissociation energy, calculated on reaction 1′ are equivalent to 107.8 kcal/mol (C_{5v}) at B3LYP/gen. Comparing the first dissociation energy with the second dissociation energy of the P_5^-−Ti−P_5^- bond, we found there is a marked difference between the first dissociation energy and the second dissociation energy of the P_5^-−Ti−P_5^- bond, which is similar to the first and second ionization energies, so the first dissociation in [Ti(η^5−P_5)$_2$]$^{2-}$ (D_{5d} and D_{5h}) is very easy, instead of the second dissociation. On the other hand, the low stability of the [Ti (η^5−P_5)$_2$]$^{2-}$ (D_{5d} and D_{5h}) toward dissociation into [Ti (η^5−P_5)]$^-$ (C_{5v}) and P_5^- comes from a strong repulsion between two P_5^- groups in the dianion, because they are too close to each other, in which the distance between the P_5^- groups is only 3.66 Å. Therefore, we conclude that [Ti (η^5−P_5)]$^-$ (C_{5v}) is more stable than [Ti (η^5−P_5)$_2$]$^{2-}$ (D_{5d} and D_{5h}).

On the basis of the frequency calculation and analysis in the staggered form, there is an imaginary frequency which indicates it is a transition state; the ring rotation barrier from the staggered [Ti (η^5−P_5)$_2$]$^{2-}$ to eclipsed [Ti (η^5−P_5)$_2$]$^{2-}$ is 5.7 kcal/mol at B3LYP/gen, and it agrees well with the predicted result (7.8 kcal/mol).[32] Although the repulsion energies between blocks P_5^- are higher in the eclipsed D_{5h} conformation than in the staggered D_{5d} conformation, which the former comes from direct ring−ring electrostatic contributions, the latter comes from indirect contribution. However, the total bond dissociation energies (ΔE_1), total binding energies (ΔE_2), and first bond dissociation energies (ΔE_5) between Ti and blocks (see below) are all higher in the former than in the latter. On one hand, it further shows that covalent bonds between Ti and blocks P_5^- are stronger in the former than in the latter. On the other hand, as Carter pointed out, the induction energy of the metal of in the potential filed of the eclipsed rings, which comes from direct ring−ring electrostatic contributions,[30(d)] is lower than in the staggered ring, which comes from indirect ring−ring electrostatic contributions. Otherwise, the reverse results are obtained. Thus, the eclipsed conformation is more stable than the staggered conformation.

B. Optimized Bond Distances and the Nature of the Metal−Ligand Interaction. Except for the trend of all bond P−P distances in the same structure being equal and intermediate between P−P single and P═P double bond distances (but there is a slight longer the P−P bond distance in [Ti (η^5−P_5)]$^-$$C_{5v}$) (2.22∼2.24 Å) than P═P double bond distance), two kinds of trends can be inferred from Table 1. One kind of trend is that the computed P−P bond distances in [Ti (η^5−P_5)]$^-$ (C_{5v}) and that in [Ti (η^5−P_5)$_2$]$^{2-}$ (D_{5d} and D_{5h})with five different methods increase in the following order: P_5^- (D_{5h}) < [Ti (η^5−P_5)$_2$]$^{2-}$ (D_{5d} and D_{5h}) < [Ti (η^5−P_5)]$^-$ (C_{5v}), in which the eclipsed form is slightly longer than the staggered form. Another is that computed bond distances between Ti and P in three kinds of species decrease in the following order: [Ti (η^5− P_5)$_2$]$^{2-}$ (D_{5d} and D_{5h}) < [Ti (η^5−P_5)]$^-$ (C_{5v}), in which the eclipsed form is slightly shorter than the staggered form.

Based on the equation of all of the P−P bond distances in the same conformation, including the increasing trend of P−P bond distance and the decreasing trend of Ti−P along with the order P_5^- (D_{5h}) < [Ti (η^5−P_5)$_2$]$^{2-}$ (D_{5d} and D_{5h}) < [Ti (η^5−P_5)]$^-$ (C_{5v}), we could conclude that building block P_5^- in all three species has a delocalized P−P bond, too, and the strength of P−P bond decease and the strength of Ti−P bond increase in the above order.

To explore the nature of the P−P bond and of interactions between Ti and building blocks P_5^- in P_5^- (D_{5h}), [Ti (η^5−P_5)]$^-$ (C_{5v}), and [Ti (η^5−P_5)$_2$]$^{2-}$ (D_{5h} and D_{5d}), the molecular orbital of three kinds of species were computed with the B3LYP/6-311++G(d,p) method,[36] and MOs pictures, which are relevant HOMOs, were exhibited in Figures 2, 3, and 5. MO correlation diagrams for the interaction between Ti and a five-membered cyclic ligand P_5^- were graphed correspondingly in Figure 4 and between two P_5^- blocks and Ti in Figure 6.

As shown in Figure 2, P_5^- (D_{5h}) possesses six π electrons occupied in three π MOs (two degenerate HOMOs and HOMO-3, the third orbital below HOMO) forming a P−P π bond and resulting in π aomaticity according to the $(4n + 2)$ π Hükcel rule. Meanwhile, cyclic σ symmetric MOs (HOMO-4 and HOMO-7) and other MOs P−P form σ bond and produce σ ring current to induce σ aromaticity. The formation of both the π and σ bonds induces P−P bond distances to become equal in P_5^- (D_{5h}) and to shorten. When Figures 3 and 5 are compared with Figure 2, the cyclic σ bond like that in P_5^- (D_{5h}) lies in then building block P_5^- of [Ti (η^5−P_5)]$^-$ (C_{5v}) (see HOMO-8 in Figure 3) and of [Ti (η^5−P_5)$_2$]$^{2-}$ (D_{5h} and D_{5d}) (see HOMO-15, HOMO-16 in Figure 5), too. Thus, the σ ring current induced by σ aromaticity in building block P_5^- results in P−P bond distances becoming equal in [Ti (η^5−P_5)]$^-$ (C_{5v}) and [Ti (η^5−

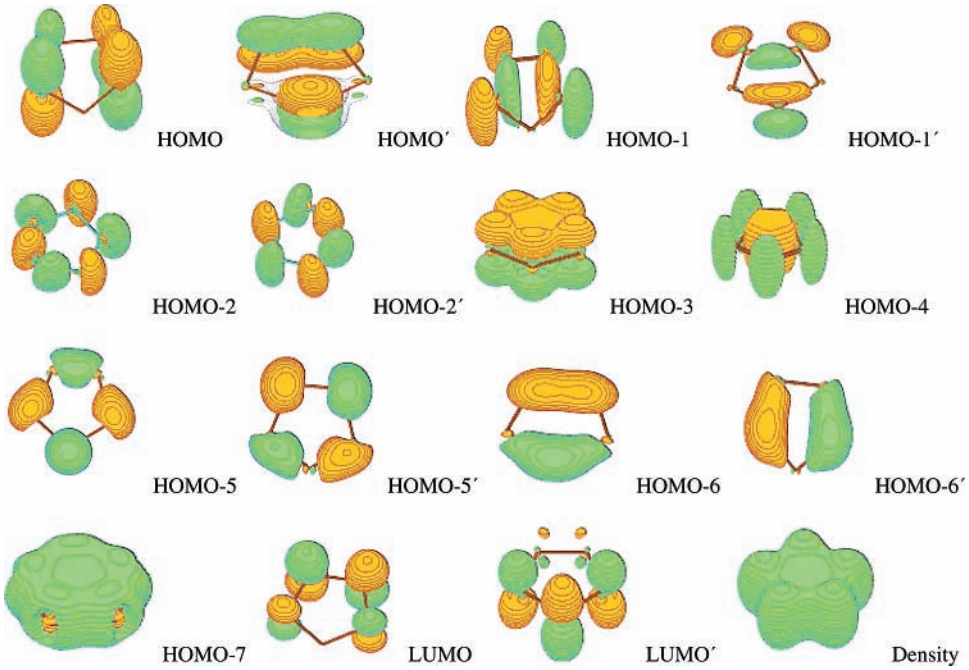

Figure 2. Pictures of molecular orbital and total density in P_5^-(D_{5h}, $^1A_1$) at B3LYP/6-311++G(d,p).

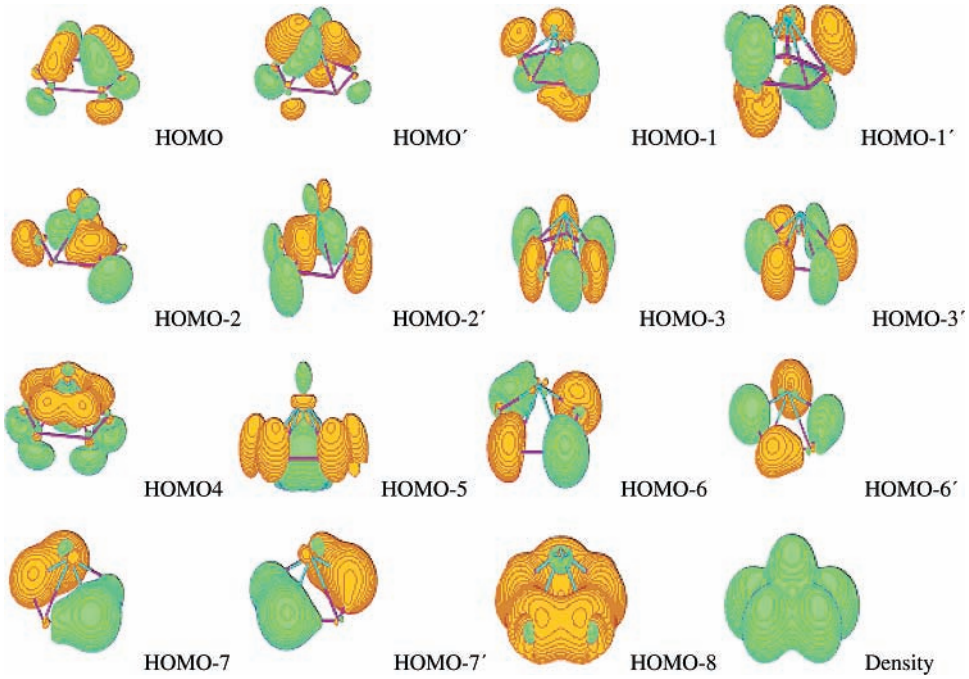

Figure 3. Pictures of molecular orbital and total density in [Ti (η^5-P_5)]$^-$(C_{5v}) at B3LYP/6-311++G(d,p).

$P_5)_2]^{2-}$ (D_{5h} and D_{5d}). However, there are distinctly some differences between [Ti (η^5-P_5)]$^-$ (C_{5v}) or [Ti ($\eta^5-P_5)_2]^{2-}$ (D_{5h} and D_{5d}) and P_5^- (D_{5h}), in which there is not a P−P π bond and there are special cyclic σ, π, and δ bonds by interaction between HOMO and LUMO in block P_5^- with the same symmetry atomic d orbital in the Ti atom. These P−P interactions in three species result in the deformation of rings which are slightly larger than that in the monoanion and larger in [Ti (η^5-P_5)]$^-$ (C_{5v}) than in [Ti ($\eta^5-P_5)_2]^{2-}$ (D_{5h} and D_{5d}).

As can be seen from Figures 3 and 4, there are three kinds of interactions between Ti and block P_5^- in the fragment [Ti (η^5-P_5)]$^-$ (C_{5v}) except for the σ bond of P−P like that in P_5^- (D_{5h}). That is the δ bond {two HOMO(e_2) in[Ti (η^5-P_5)]$^-$ (C_{5v})} as a result of interaction of the δ symmetry degenerate LUMO in block P_5^- with the same symmetry degenerate occupied atomic orbitals d_{xy} and $d_{x^2-y^2}$ in Ti atom and the π bond {two HOMO-2(e_1) in [Ti (η^5-P_5)]$^-$ (C_{5v})} resulting from the interaction π symmetry degenerate HOMO in block P_5^- with the same symmetry degenerate unoccupied atomic orbital d_{xz} and d_{yz} in the Ti atom, and σ bond {HOMO-4(a′) and HOMO-5(a) in [Ti (η^5-P_5)]$^-$ (C_{5v})} induced by interaction σ symmetry occupied HOMO-3(a_1) and HOMO-4(a_2) in block P_5^- with the same symmetry unoccupied atomic orbital d_{z^2} in Ti atom. Comparing Figures 5 and 6 with Figures 3 and 4, correspondingly, we found that interactions of the δ, π, and σ bonds between Ti and block P_5^- in [Ti ($\eta^5-P_5)_2]^{2-}$ (D_{5h} and D_{5d}) are analogous to that in [Ti (η^5-P_5)]$^-$ (C_{5v}). Based on analysis of the contributions of Ti− P_5^- bonding in [Ti ($\eta^5-P_5)_2]^{2-}$, with the ETS method by Lein,[33] which showed that the contributions of σ, π, and δ bonding are 10.7%, 31.5%, and 57.8%,

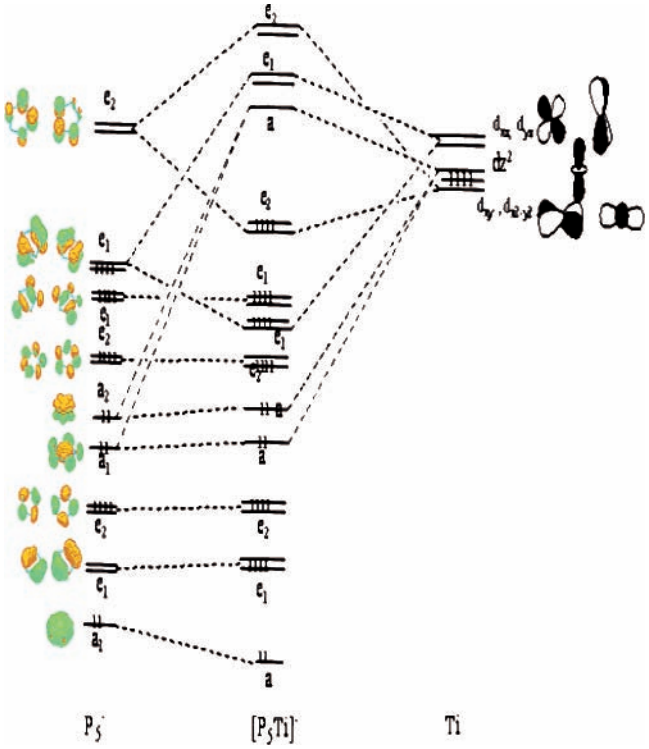

Figure 4. MO correlation diagram for the interaction between Ti and P_5^- block in [Ti (η^5-P_5)]$^-$(C_{5v}).

respectively, the dominant orbital interactions come from the Ti → [(η^5-P_5)$_2$]$^{2-}$ back-donation δ bonding. However, it was concluded that, after inspection and comparison of Ti−P bond distances which are longer in [Ti (η^5-P_5)$_2$]$^{2-}$ (D_{5h} and D_{5d}) than in [Ti (η^5-P_5)]$^-$ (C_{5v}), the interactions between Ti and block P_5^- in moiety of [Ti (η^5-P_5)$_2$]$^{2-}$ (D_{5h} and D_{5d}) are not stronger than that in [Ti (η^5-P_5)]$^-$ (C_{5v}).

To contrast the strength of the Ti−P bond in [Ti (η^5-P_5)]$^-$ (C_{5v}) with that in [Ti (η^5-P_5)$_2$]$^{2-}$ (D_{5h} and D_{5d}), energetic analysis was carried out according to hypothetical reactions 1, 1′, and 2−5. Based on reaction 1, we calculated the total P_5^-−Ti−P_5^- dissociation energies (ΔE_1), and further calculated an average Ti−P_5^- dissociation energy ($^1/_2\Delta E_1$) in [Ti (η^5-P_5)$_2$]$^{2-}$ (D_{5h} and D_{5d}), which are equivalent to 59.0 kcal/mol (D_{5h}) and 56.1 kcal/mol (D_{5d})) at B3LYP/gen, respectively, whereas Ti−P_5^- dissociation energies in [Ti (η^5-P_5)]$^-$ (C_{5v}) calculated on reaction 1′ are equivalent to 107.8 kcal/mol (C_{5v}) at B3LYP/gen. In parallel, we calculated total P_5^-−Ti−P_5^- total binding energies (ΔE_4) based on reaction 4, in which the Ti atom is pulled out of the equilibrium geometry of [Ti (η^5-P_5)$_2$]$^{2-}$ (D_{5h} and D_{5d}), and we further calculate average Ti−P_5^- binding energies ($1/2\Delta E_4$) which are equivalent to 99.6 kcal/mol (D_{5h}) and 107.4 kcal/mol (D_{5d}) at B3LYP/gen, respectively, whereas the Ti−P_5^- binding energies calculated on analogous reaction 1′, in which the Ti atom is pulled out of the equilibrium geometry of [Ti (η^5-P_5)]$^-$ (C_{5v}), are equivalent to 119.6 kcal/mol (C_{5v}) at B3LYP/gen. Comparing these reaction energies, we conclude that the Ti−P bond in [Ti (η^5-P_5)]$^-$ (C_{5v}) is stronger than that in [Ti (η^5-P_5)$_2$]$^{2-}$ (D_{5h} and D_{5d}). The same conclusion is supported by the calculated result with B3LYP/6-311++G(d,p) (see the Supporting Information).

The reason that P−P bond distances slightly shorten in [Ti (η^5-P_5)$_2$]$^{2-}$ (D_{5d}) than in [Ti (η^5-P_5)$_2$]$^{2-}$ (D_{5h}) is because the strengthening of the Ti− P_5^- bond in [Ti (η^5-P_5)$_2$]$^{2-}$ (D_{5h}) slightly than in [Ti (η^5-P_5)$_2$]$^{2-}$ (D_{5d}) leads to the weakening of the P−P bond of blocks P_5^- in [Ti (η^5-P_5)$_2$]$^{2-}$ (D_{5h}) than [Ti (η^5-P_5)$_2$]$^{2-}$ (D_{5d}), which the electronic densities of P−P bond of blocks P_5^- are more concentrated on Ti−P_5^- in [Ti (η^5-P_5)$_2$]$^{2-}$ (D_{5h}) than in [Ti (η^5-P_5)$_2$]$^{2-}$ (D_{5d}). Thus, P−P bond distances of block P_5^- are slightly shorter in [Ti (η^5-P_5)$_2$]$^{2-}$ (D_{5d}) than in [Ti (η^5-P_5)$_2$]$^{2-}$ (D_{5h}).

C. Aromaticity. Figure 1 and Table 1 show that every stable form in all kinds of species for planar ring P_5^- (D_{5h}), [Ti (η^5-P_5)]$^-$ (C_{5v}), and [Ti (η^5-P_5)$_2$]$^{2-}$ possess planar five cyclic block P_5^-, and an equivalent P−P bond length, whose characteristics are well in agreement with the criterion of aromatic geometry. Further calculated numbers of conjugated π electron in block P_5^- agree with the Hückel's rule of $4n + 2$ π electrons. However, it is worthy of further study whether the aromaticities of the three species are in agreement with the criterion of NICS, and how many the NICS, which orders of aromaticity, what are the relations between the NICS values and all of the kinds of bond NICS contributions, and so on. Wherefore, the calculated NICSs of the optimized structures, at the ring center 1 Å above the ring center and minimum NICS beneath the ring center, are listed in Table 3, and the curves of total NICSs distribution, and of dissected total NICS, into all kinds of bond NICS, at 0.25 Å successions of points from the P_5 ring center using GIAO−B3LYP/gen method, were plotted in Figures 7−11.

To search for the best method on computing NICS, six methods were used to compute the NICS for P_5^- (D_{5h}) as listed in Figure 7. The results of the six methods are similar. The NICSs are slightly high at GIAO−HF/6-311+G(2d)//HF/6-311+G(2d) and slightly low at GIAO−B3LYP/6-311++G(d, p)//B3LYP/6−311++G(d, p). By further researching, we found the results at GIAO−B3LYP/6-311+G(2d)//B3LYP/6-311+G-(2d) are the more reliable, lying in the middle between the two methods.

To check the computational reliability, the NICSs for benzene were computed with GIAO−B3LYP/6-311+G(2d)//B3LYP/6-311+G(2d). The calculated NICSs on benzene show that our results, NICS(0) = −7.6(ppm) and NICS(1) = −10.1(ppm), are in good agreement with the previously computed ones (NICS(0) = −8.8(ppm) and NICS(1) = −10.6(ppm).[37] It means that our computed methods are reliable.

1. Aromaticity of the Planar P_5^- Anion. As listed in Table 3, the NICS(0) and NICS(1) for planar ring P_5^- (D_{5h}) anion is more negative than those of benzene, i.e. P_5^- (D_{5h}) is more aromatic than benzene. As shown in Figure 2, P_5^- (D_{5h}) possesses six π electrons occupied in three π MOs resulting in π aromaticity according to $(4n + 2)$ π Hükcel's rule. To research to how many NICS contributions a various bond, and to look for the correlations between contributions of bond NICS values and the total NICS values in P_5^- (D_{5h}), we dissected the total NICS values into all kinds of bond NICS values, including NICS components of the P−P π and P−P σ bonds and of core and lone pair electron(neglected in Figure 8), and the results are shown in Figure 8.

Comparing dissected NICS contributions of P_5^- with that of benzene in ref 37, we found that there are both similarities and differences between two kinds plots in Figure 8 and in ref 37. On one hand, both plots are very similar: with the distance increasing, the curves of NICS contribution of the σ bond all drop off, while of total NICS and of π bond rise up, and of core and lone pair electrons are near invariable, and the changing trends of curve of total NICS are consistent with of the curves of NICS contribution of π bond, are dominated by NICS contribution of π bond. On the other hand, both NICS components of P−P π bond and NICS components of P−P σ

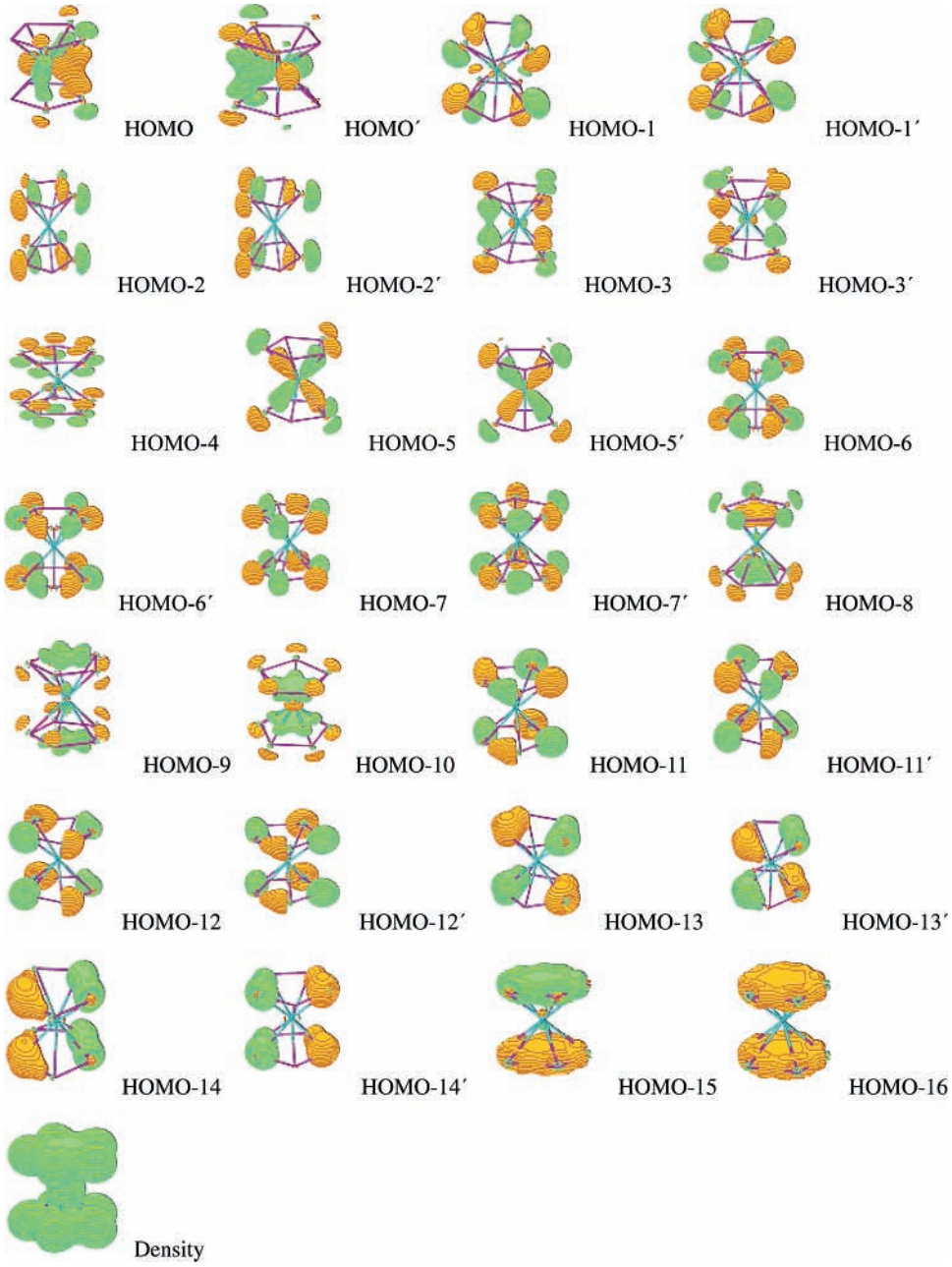

Figure 5. Pictures of molecular orbital and total density in eclipsed [Ti (η^5-P_5)$_2$]$^{2-}$ (D_{5h}) at B3LYP/6-311++G(d,p).

bond in P_5^- anion are negative. Although NICS components of the C−C π bond is negative, NICS components of C−C σ bond in benzene is positive.[37] So P_5^- (D_{5h}) is more aromatic than benzene. This is consistent with that planar ring P_5^- (D_{5h}) anion has large binding energy listed in Table 3. Meanwhile, the positions and values of the lowest NICS(total) are different, for benzene lowest NICS(1.0) = −10.1(ppm) at B3LYP/gen, and for P_5^- lowest NICS(0.5) = −15.7(ppm) at the same level.

2. Aromaticity of the Fragment [Ti (η^5−P_5)]$^-$. As shown in Table 3, NICS(0) and NICS(1) for fragment [Ti (η^5−P_5)]$^-$ (C_{5v}) are more negative than those of P_5^- (D_{5h}), and the large values of NICS(0) and NICS(1) indicate the enormous enhancement of the σ-aromaticity and of the π−aromaticity of the P_5^- rings of [Ti (η^5−P_5)]$^-$. To distinguish the different aromaticity between fragments [Ti(η^5−P_5)]$^-$ (C_{5v}) and P_5^- (D_{5h}), we studied the distribution pattern of NICSs for [Ti (η^5−P_5)]$^-$ (C_{5v}) in the outer (called as o-total NICS) and in the inner of plane (called as i-total NICS) of P_5^- rings of [Ti (η^5−P_5)]$^-$. The distributions of total NICS in [Ti (η^5−P_5)]$^-$ and in P_5^- at different points were plotted in Figure 9.

As can be seen from Figure 8, two differences could be found. First, although the distribution of total NICS in outer of plane of P_5^- rings of [Ti (η^5−P_5)]$^-$ are similar to that of P_5^- anion except that the NICS values of the former are more negative than the latter, which the total NICS curve rises up along with increasing of the distances from the point to the center of P_5^- rings, the curve of the former does not has a minimum point while the latter has the minimum point. Second, except that the total NICS values in inner of plane of P_5^- rings of [Ti (η^5−P_5)]$^-$ are very more negative than that of P_5^- anion, and then that in outer of plane of P_5^- rings of [Ti (η^5−P_5)]$^-$, the total NICS curve has a minimum point (the smallest total NICS (0.25 Å) = −78.1 ppm), which a distances from the point to the center of P_5^- rings is 0.25 Å, and change very much deeply. It means that NICS in inner side of P_5^- ring is very sensible to its position, the nearer to Ti which is from the center

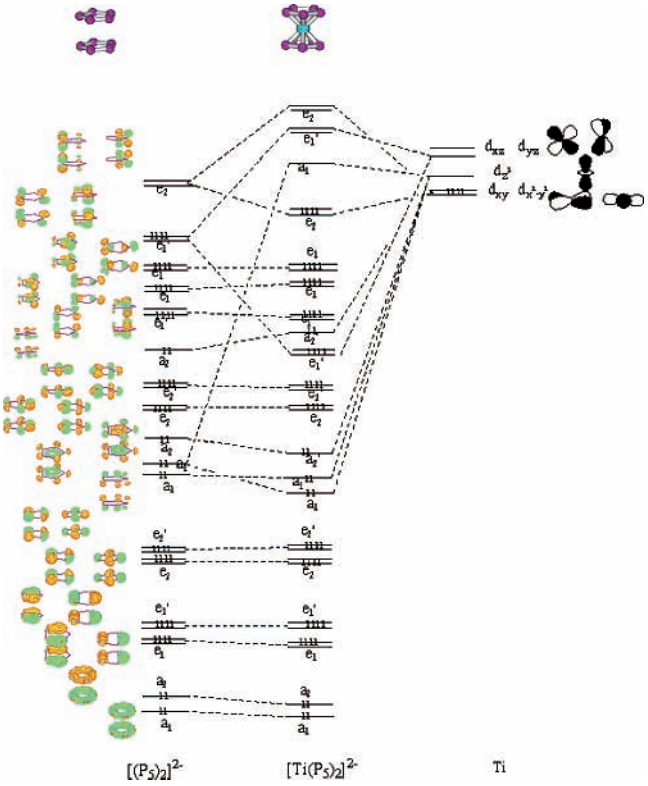

Figure 6. Orbital correlation diagram of the interactions between Ti atom (d^4) and $[(\eta^5\text{-}P_5)-(\eta^5\text{-}P_5)]^{2-}$ ligand in $[Ti(\eta^5\text{-}P_5)_2]^{2-}$ (D_{5h}).

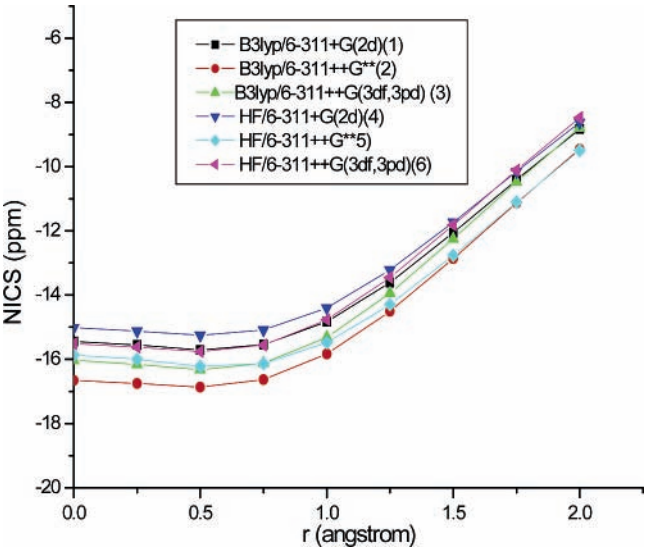

Figure 7. Distributions of total NICS for $P_5^-(D_{5h}, {}^1A_1)$ with distance between ring planar center to points above center at different methods.

of P_5^- rings 1.43 Å, the more positive NICS is, and the stronger local antiaromaticity. These differences are responsible for the difference of bonding, which there are three kinds of chemical bonds—σ, π, and δ bonds—in the fragment [Ti $(\eta^5-P_5)]^-$ while there are only two types of bonds—σ, π, bonds—in P_5^- anion. As the detail analysis, it can be made reference to the discussion of dissected NICS for P_5^- and [Ti $(\eta^5-P_5)_2]^{2-}$.

Figure 9 shows that there are differences between the total NICS curve in outer side point of the P_5^- plane and in inner side point of the P_5^- plane for [Ti $(\eta^5-P_5)]^-$, which outer-total NICS curve rises with the increasing of distances, and there is no minimum point, but there is a minimum point at $r = 0.25$ Å for inner-NICS curve, where the minimum NICS is −78.1 ppm. Therefore, we can conclude that the local aromaticity and local

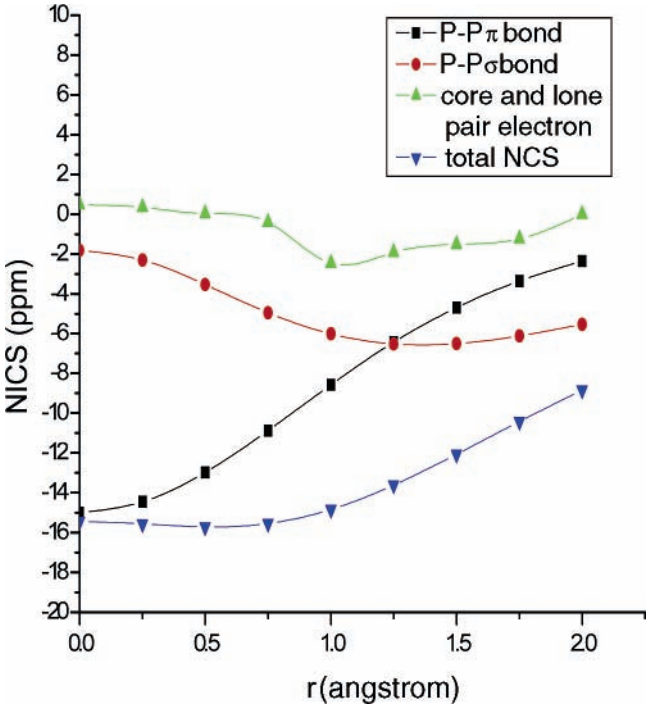

Figure 8. Plot of the NICS contributions of various bonds, and total NICS distribution at the ring center of $P_5^-(D_{5h})$ up to 2.0 Å above at B3LYP/6-311+G(2d).

aromatic distribution are complete different between the outer side point of the P_5^- plane and the inner side point of the P_5^- plane in the fragment [Ti $(\eta^5-P_5)]^-$.

3. Aromaticity of the Sandwich Complexes [Ti $(\eta^5-P_5)_2]^{2-}$. There are several trends one can infer from Table 3. First of all, NICSs of [Ti $(\eta^5-P_5)_2]^{2-}$ (D_{5h} or D_{5d}) moiety are more negative than those of P_5^- anion, and much less negative than those of [Ti $(\eta^5-P_5)]^-$ (C_{5v}). For example, the exaltations of NICS(0) and NICS(1) for [Ti $(\eta^5-P_5)_2]^{2-}$ (D_{5h}) relative to the P_5^- anion at the B3LYP/gen level are −21.4 and −6.2 ppm, correspondingly, whereas the exaltations are not as small as that of [Ti $(\eta^5-P_5)]^-$ (C_{5v}), in which the exaltations are −57.7 and −19.6 ppm, correspondingly. The minimum NICS underneath the ring center of inner side of the P_5^- plane for [Ti $(\eta^5-P_5)_2]^{2-}$ (D_{5h} or D_{5d}) is much less negative than that of [Ti $(\eta^5-P_5)]^-$ (C_{5v}) (see Table 3). Therefore, the total NICS in the outer and inner plane of ring center denotes that the local aromaticity of [Ti $(\eta^5-P_5)_2]^{2-}$ (D_{5h} or D_{5d}) is larger than that of the P_5^- anion but smaller than that of [Ti $(\eta^5-P_5)]^-$ (C_{5v}).

The total NICS distributions and the NICS contributions of various bonds for total NICS at 0.25 Å successions of points (as shown in Figures 10 and 11) above the ring center of the outer side of the P_5^- plane and underneath the ring center of the inner side of the P_5^- plane for [Ti $(\eta^5-P_5)_2]^{2-}$ (D_{5h} or D_{5d}) might further highlight the subtlety of the P_5^- ring current behavior in eclipsed [Ti $(\eta^5-P_5)_2]^{2-}$ or staggered [Ti $(\eta^5-P_5)_2]^{2-}$.

First, by comparing the NICS values in the outer of plane in the [Ti $(\eta^5-P_5)_2]^{2-}$ (D_{5h} or D_{5d}) moiety with in P_5^- (D_{5h}) anion (see Table 3), we found that total NICS values in former are more negative in the later, for example, NICS(0) and NICS-(1.0) in former (D_{5h}) are −36.8 and −21.1 ppm, respectively, whereas NICS(0) and NICS(1.0) are −15.4 and and −14.8 ppm, respectively. So the [Ti $(\eta^5-P_5)_2]^{2-}$ (D_{5h} or D_{5d}) moiety is more aromatic than P_5^- (D_{5h}) anion. At the same time, by comparing total NICS distributions of the outer plane in the [Ti $(\eta^5-P_5)_2]^{2-}$ (D_{5h} or D_{5d}) moiety with the P_5^- (D_{5h}) anion (see Figure 10,

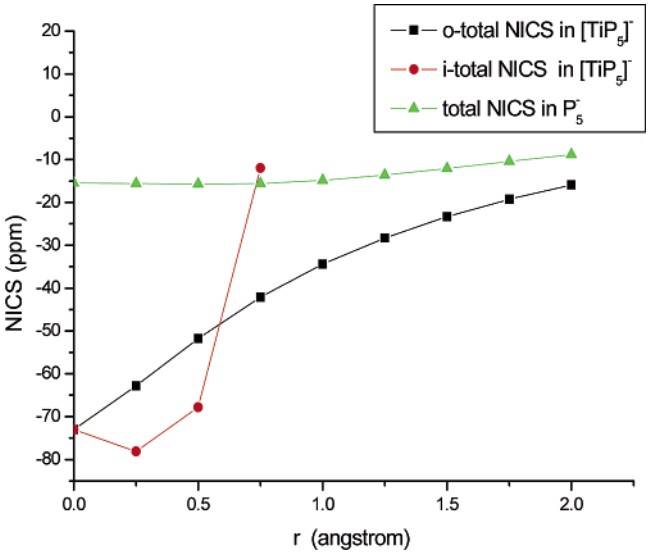

Figure 9. Total NICS distributions in [Ti (η^5-P_5)]$^-$ and in P_5^- (D_{5h}) with distance between ring planar center to points outer and inner ring plane at B3LYP/6-311+G(2d).

panels a and b), we found that the distributions of total NICS in two cases are different, which the total NICS curve of the outer side point of the P_5^- plane for the [Ti (η^5−P_5)$_2$]$^{2-}$(D_{5h} or D_{5d}) moiety rises with the increasing of distances, whereas although the total NICS curve for P_5^- anion rises up, too, there is a minimum point. It implies that the distributions of aromaticity in the two cases are slightly different, in which the aromaticity of the P_5^- anion has the largest region at $r = 0.75$ Å, but the aromaticity of the outer side of the P_5^- plane for the [Ti (η^5−P_5)$_2$]$^{2-}$ (D_{5h} or D_{5d}) moiety has not this region. Second, by the same comparison, we found that the NICS value of the inner side and that near to the P_5^- plane for the [Ti (η^5−P_5)$_2$]$^{2-}$ (D_{5h} or D_{5d}) moiety is much more negative than that of the P_5^- plane; for example, the minimum NICS for the former is NICS(0.75) = −45.8 ppm((D_{5h}), whereas the minimum NICS for the latter is only NICS(0.75) = −15.7 ppm. It adequately implies that the aromaticity in the inner side and that near to the P_5^- plane for [Ti (η^5−P_5)$_2$]$^{2-}$ (D_{5h} or D_{5d}) moiety is larger than that of the P_5^- anion and larger than that of the outer side of the P_5^- plane for the [Ti (η^5−P_5)]$^{2-}$ (D_{5h} or D_{5d}) moiety. Meanwhile, the distributions of total NICS in two cases are obviously different, which, with the increasing of distances, the total NICS curve of the inner side point of the P_5^- plane for the [Ti (η^5−P_5)$_2$]$^{2-}$ (D_{5h} or D_{5d}) moiety is markedly concave, wereas that of the P_5^- anion is slightly concave, and the nearer the computed point to the Ti atom of the molecular center in [Ti (η^5−P_5)$_2$]$^{2-}$ (D_{5h} or D_{5d}) is, the more positive the NICS value is. So we can infer that the region near to the Ti atom (at $r = 1.84$ Å) in [Ti (η^5−P_5)$_2$]$^{2-}$(D_{5h} or D_{5d}) is antiaromaticity (see Figure 10). Third, Figure 10 shows that there are differences between the total NICS in the curve of the outer side of the P_5^- plane and in the inner side of the P_5^- plane for [Ti (η^5−P_5)$_2$]$^{2-}$ (D_{5h} or D_{5d}), where the outer-total NICS curve rises with increasing distances. Also, there is no minimum point, but there is a minimum point at $r = 0.75$ Å for inner-NICS curve, where the minimum NICS is −45.8 ppm (D_{5h}), and the NICS of inner side and near to the P_5^- plane is more negative than that of the outer side of the P_5^- plane. So we can conclude that the local aromaticity and local aromatic distribution are completely different between the outer side point of the P_5^- plane and the inner side point of the P_5^- plane for the [Ti (η^5−P_5)$_2$]$^{2-}$ (D_{5h} or D_{5d}) moieties, which the local aromaticity in the inner side

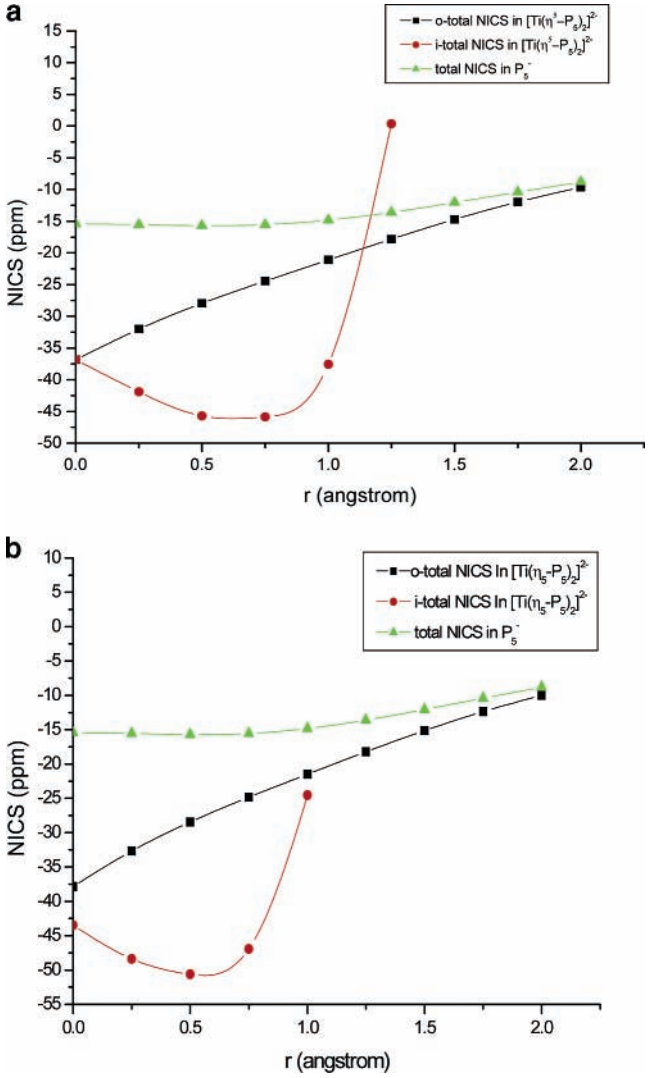

Figure 10. Total NICS distribution in [Ti (η^5-P_5)$_2$]$^{2-}$ and in P_5^-(D_{5h}) with distance between ring planar center to points outer and inner ring plane at B3LYP/6-311+G(2d) (a) eclipsed form (D_{5h}), (b) staggered form (D_{5d}).

point of the P_5^- plane is much stronger than that of the outer side point of the P_5^- plane.

As for the reason that the local aromaticity of the eclipsed [Ti (η^5−P_5)$_2$]$^{2-}$ moiety is larger than that of the P_5^- anion, it is an important reason that interactions between Ti and block P_5^- in eclipsed [Ti (η^5−P_5)$_2$]$^{2-}$ inducing to δ, π, and σ bonds as above discussion enhance the local aromaticity of eclipsed [Ti (η^5−P_5)$_2$]$^{2-}$ moiety and change in the distribution of the total NICS. To check it, we computed the various NICS contributions at the ring center of P_5^-in [Ti (η^5-P_5)$_2$]$^{2-}$ up to 2.0 Å above or down to 1.5 Å beneath at B3LYP/6-311+G(2d), including the P−P π bond NICS, the P−P σ bond NICS, and the P_5−Ti bond NICS (the sum of the π, δ, and σ bonds NICS contribution), and Ti and all of P lone pair electron. Two plots of the various contributions are shown in Figure 11. As shown from Figure 11, we found that, whether out of plane or in plane, the P−P π bond contribution and the P_5−Ti bond contribution which are negative are exceptionally larger and dominate the P−P σ bond and the Ti and P lone pair electron contributions, which predominate over the total NICS. The resulting uniquely large diatropic total denotes the aromaticity of [Ti(η^5-P_5)$_2$]$^{2-}$. Contrasting the NICS contributions of P−P π and σ bonds in the P_5^- anion with in [Ti(η^5-P_5)$_2$]$^{2-}$, it is only the difference that there is a P_5−Ti bond contribution induced by the σ, π, and δ

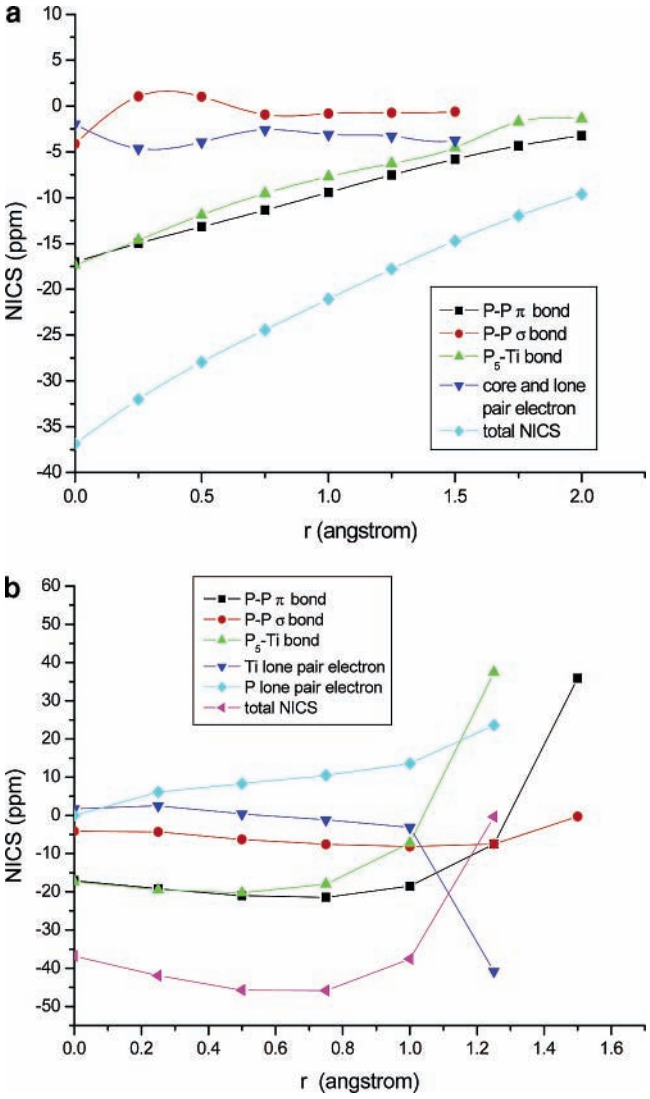

Figure 11. Plot of the various NICS contributions at the ring center of P_5^- in [Ti (η^5-P_5)$_2$]$^{2-}$ up to 2.0 Å above, or down to 1.5 Å beneath at B3LYP/6-311+G(2d) (a) out of plane of P_5^-, (b) inner of plane of P_5^-.

bonds between P_5^- and Ti. Thus, the P_5−Ti bond contribution for total NICS is a dominant factor that the aromaticity of [Ti(η^5-P_5)$_2$]$^{2-}$ is stronger.

Furthermore, when Figures 10 and 11 are compared, the changing trends of the NICS contribution of the P−P π bond and of the P_5−Ti bond are consistent with the trend of total NICS, rising up. However, the changing trends of the NICS contribution of the P−P σ bond and of the lone pair electron are largely cancaled by the NICS contribution of the P−P π bond and of the P_5−Ti bond. Thus, we conclude that the π bond, including the bond combining nonmetal with nonmetal and with metal, mostly induces the production of a diatropic current, which results in the π aromaticity, that the σ bond and the lone pair electron mostly induce the production of a paratropic current, which results in the σ antiaromaticity, and that the molecular total aromaticity depends on the sum of NICS contributions all kinds of bonds.[37,39]

Comparing Figure 10 with Figure 9, we can find that the changing trends of total NICS curves for fragment [Ti (η^5−P_5)]$^-$ (C_{5v}) are almost the same as those for the [Ti (η^5−P_5)$_2$]$^{2-}$ (D_{5h} or D_{5d}) moiety except for the total NICS in magnitude being much smaller, the minimum NICS values and positions of minimum NICS underneath the ring center of inner side of

TABLE 4: Nucleus Independent Chemical Shift (NICS) Values for P_5^-, Eclipsed [(η^5-P_5)-(η^5-P_5)]$^{2-}$(D_{5h}) and Staggered [(η^5-P_5)-(η^5-P_5)]$^{2-}$(D_{5d}) at the B3LYP/gen Level

species	sym		NICS(0)	NICS(1)	center
P_5^-	D_{5h}		−15.4	−14.8	
[(η^5−P_5)−(η^5−P_5)]$^{2-}$	D_{5h}	*a*	−8.5 [c]	−12.3[c]	−4.9
		b		−7.2[c]	
[(η^5−P_5)−(η^5−P_5)]$^{2-}$	D_{5d}	*a*	−10.6[d]	−12.9[d]	−8.3
		b		10.3[d]	

[a] Outer plane. [b] Inner plane. [c] Computed at the geometric reference of eclipsed [(η^5−P_5)−(η^5−P_5)]$^{2-}$(D_{5h}): r(P−P) = 2.175 Å, r(P^5−P_5) = 3.669 Å. [d] Computed at the geometric reference of staggered [(η^5−P_5)−(η^5−P_5)]$^{2-}$(D_{5d}): r(P−P) = 2.169 Å, r(P^5−P_5) = 3.724 Å.

P_5^- plane. The minimum for fragment [Ti (η^5−P_5)]$^-$ (C_{5v}) underneath the ring center of the inner side of the P_5^- plane is the total NICS equal to −78.1 ppm, and its position is at r = 0.25 Å. This minimum NICS is much smaller than that of the [Ti (η^5−P_5)$_2$]$^{2-}$ (D_{5h} or D_{5d}) moiety. Hence, these results reveal further that the local aromaticity of the fragment [Ti (η^5−P_5)]$^-$ (C_{5v}) is larger than that of the [Ti (η^5−P_5)$_2$]$^{2-}$ (D_{5h} or D_{5d}) moiety. As for the reason, it is because interactions between Ti and block P_5^- in fragment [Ti (η^5−P_5)]$^-$ (C_{5v}) inducing to δ, π, and σ bonds as in the above discussion are much stronger than that of the eclipsed [Ti (η^5−P_5)$_2$]$^{2-}$ (D_{5h} or D_{5d}) moiety. Another reason is that there are repulsions between P_5^- blocks in [Ti (η^5−P_5)$_2$]$^{2-}$ (D_{5h} or D_{5d}).

Comparing panela a and b in Figure 10 and the NICS values of the eclipsed form with the staggered form for the [Ti (η^5−P_5)$_2$]$^{2-}$ moiety (see Table 3), we found that the total NICS in magnitude, distribution of total NICS, and dissection of NICS contributions of the bond for the eclipsed and staggered forms (neglected the plots of the various NICS contributions of bond) are almost the same. However, there are some tiny differences between the eclipsed (D_{5h}) and staggered conformation forms (D_{5d}), too. As shown Table 3, NICS(0), NICS(1), and minimum NICS of inner side of P_5^- plane for the eclipsed form are not as negative as those of the staggered form at the same calculating levels. These results show that the local aromaticity of the staggered [Ti (η^5−P_5)$_2$]$^{2-}$ moiety in magnitude is slightly larger than that of the eclipsed [Ti (η^5−P_5)$_2$]$^{2-}$ moiety.

To explore the mystery of why the NICSs of the staggered [Ti (η^5−P_5)$_2$]$^{2-}$ moiety in magnitude is slightly larger than that of the eclipsed [Ti (η^5−P_5)$_2$]$^{2-}$ moiety, we computed the NICSs of two unstable imaginary geometric structures which were taken away the Ti atom from the equilibrium structures of eclipsed [Ti (η^5−P_5)$_2$]$^{2-}$ (D_{5h}) and of staggered [Ti (η^5−P_5)$_2$]$^{2-}$ (D_{5d}), and frozen other P atom positions as that of the equilibrium structures, called eclipsed [(η^5−P_5)−(η^5−P_5)]$^{2-}$ (D_{5h}) and staggered [(η^5−P_5)−(η^5−P_5)]$^{2-}$ (D_{5d}), respectively. The NICS-(0), NICS(1), and NICS(−1) (the NICS of inner side point of P_5^- plane at r = 1.0 Å) in eclipsed [(η^5−P_5)−(η^5−P_5)]$^{2-}$ (D_{5h}) and staggered [(η^5−P_5)−(η^5−P_5)]$^{2-}$ (D_{5d}) are listed in Table 4.

Table 4 shows that the magnitudes of NICS(0), NICS(1), and NICS (−1) (see Table 4, b row results) for staggered [(η^5−P_5)−(η^5−P_5)]$^{2-}$ (D_{5d}) are slightly larger than that of eclipsed [(η^5−P_5)−(η^5−P_5)]$^{2-}$ (D_{5h}). Based on the analysis of distances between the P_5^- block and P_5^- block, which r(P_{5-} $_{P5}$) in staggered [(η^5−P_5)−(η^5−P_5)]$^{2-}$ (D_{5d}) is slightly longer than in eclipsed [(η^5−P_5)−(η^5−P_5)]$^{2-}$ (D_{5h}), we infer that the interaction of repulsion between the P_5^- block and P_5^- block in staggered [(η^5−P_5)−(η^5−P_5)]$^{2-}$ (D_{5d}) is slightly less strong than in eclipsed [(η^5−P_5)−(η^5−P_5)]$^{2-}$ (D_{5h}). Therefore, we conclude, just in the homologous status of covalent interactions, that the

smaller the electrostatic repulsion between the P_5^- blocks is, the larger the local aromaticity of the ring P_5^- blocks is.

In the homologous bonding status between eclipsed [Ti ($\eta^5-P_5)_2]^{2-}$(D_{5h}) and staggered [Ti ($\eta^5-P_5)_2]^{2-}$ (D_{5d}), we infer from the fact that r_{Ti-P} of the eclipsed form is smaller than that of the staggered form (see Table 1) that the electrostatic repulsion between two P_5^- blocks in the eclipsed form is slightly stronger than in the staggered form, so the local aromaticity of eclipsed [Ti ($\eta^5-P_5)_2]^{2-}$(D_{5h}) is slightly smaller than that of staggered [Ti ($\eta^5-P_5)_2]^{2-}$ (D_{5d}). As for the relations between the local aromaticity and the stability, it is deserving of further studying.

IV. Conclusion

The equilibrium geometries, energies, harmonic frequencies and NICSs of P_5^- (D_{5h}) anion, the fragment [Ti ($\eta^5-P_5)]^-$ (C_{5v}), and the sandwich compounds [Ti($\eta^5-P_5)_2]^{2-}$ (D_{5h} and $D_{5d,}$) are computed at the B3LYP/gen level. The energetic and detailed NICS analyses have been carried out for P_5^- (D_{5h}), [Ti ($\eta^5-P_5)]^-$ (C_{5v}) and [Ti($\eta^5-P_5)_2]^{2-}$ (D_{5h}, D_{5d}). Based on these calculations and analysis, the results of this work can be summarized as follows:

1. In each of the three structures, the P−P and Ti−P bond distances are perfectly equal, five P atoms in block P_5^- lie in the same plane, and it completely meets with the geometric criterion of aromaricity. Also, the P−P bond distance increases and the Ti−P bond distance decreases with the order P_5^-, [Ti($\eta^5-P_5)_2]^{2-}$, and [Ti ($\eta^5-P_5)]^-$.

2. The binding energy analysis, which is carried out according to the energy change of hypothetic reactions of the three species, predicts that the three species are all very stable. And further theoretical analysis of dissociation energy shows that the stability of [Ti($\eta^5-P_5)]^-$ is so stable, more stable than P_5^- and [Ti($\eta^5-P_5)_2]^{2-}$ synthesized in experiment, that could be synthesized.

3. NICS values, computed for the anion and moiety of the three species with the GIAO−B3LYP and GIAO−HF methods, reveal that three species all have a larger aromaticity, and NICS (0) of moiety, NICS(1) of moiety, and minimum NICS of inner side of ring P_5 plane in magnitude increase with the order P_5^-, [Ti($\eta^5-P_5)_2]^{2-}$, and [Ti ($\eta^5-P_5)]^-$. By analysis of binding energetic and the molecular orbital (MO) and qualitative MO correlation diagram, and the dissection of total NICS, dissected as NICS contributions of various bonds, it is the main reason for P_5^- (D_{5h}) having the larger aromaticity that the P−P σ, and π bonds have the larger diatropic ring currents in which NICS contribution are negative, specially P−P σ bond. However, in [Ti ($\eta^5-P_5)]^-$ (C_{5v}) and [Ti($\eta^5-P_5)_2]^{2-}$ (D_{5h}, and D_{5d}), the reason is the larger and more negative diatropic ring currents in which the NICS contributions of P−P π bonds and P_5−Ti bonds including π, δ, and σ bonds, especially P_5−Ti bonds, are much more negative and canceled the NICS contributions of P and Ti core and lone pair electrons.

Acknowledgment. This work was supported by the National Nature Science Foundation of China (No.20473031) and the Key Laboratory for Supramolecular Structure and Material of Jilin University.

Supporting Information Available: Optimized geometric structures, bonding distances, total energies, and the number of imaginary frequencies and NICSs for the P_5^- anion, [Ti ($\eta^5-P_5)]^-$, and [Ti($\eta^5-P_5)_2]^{2-}$ were computed with four other methods: B3LYP/6-311++G(d,p), B3LYP/6-311++G(3df,-3pd), HF/6-311++G(d,p), and HF/gen(P:6-311+G(2d), Ti:6-311+G(2df)). The same results at different levers were obtained as those at the B3LYP/gen P:6-311+G(2d), Ti:6-311+G(2df)). This material is available free of charge via the Internet at http://pubs.acs.org.

References and Notes

(1) Schleyer, P. v. R.; Jiao, H. *Pure Appl. Chem.* **1996**, *68*, 209.
(2) Li, X.; Kuznetsov, A. E.; Zhang, H.-F.; Boldyrev, A. I.; Wang, L.-S. *Science* **2001**, *291*, 859.
(3) Seo, D. K.; Corrbellt, J. D. *Science* **2001**, *291*, 841.
(4) (a) Boldyrev, A. I.; Kuznetsov, A. E. *Inorg. Chem.* **2002**, *4*, 532. (b) Jusélius, J.; Straka, M.; Sundholm, D. *J. Phys. Chem. A* **2001**, *105*, 10795. (c) Kuznetsov, A. E.; Boldyrev, A. I.; Zhai, H.-J.; Wang, L.-S. *J. Am. Chem. Soc.* **2002**, *124*, 11791. (d) Fowler, P. W.; Havenith, R. W. A.; Steiner E. *Chem. Phys. Lett.* **2001**, *342*, 85. (e) Fowler, P. W.; Havenith, R. W. A.; Steiner, E. *Chem. Phys. Lett.* **2002**, *359*, 530. (f) Zhan, C. G.; Zheng, F.; Dixon, D. A. *J. Am. Chem. Soc.* **2002**, *124*, 14795. (g) Masui, H.; *Cooord. Chem. Rev.* **2001**, *219*−*221*, 957.
(5) Kuznetsov, A. E.; Boldyrev, A. I.; Li, X.; Wang, L.-S. *J. Am. Chem. Soc.* **2001**, *123*, 8825.
(6) Alexandrova, A. N.; Boldyrev, A. I. *J. Phys. Chem. A.* **2003**, *107*, 554.
(7) (a) Kuznetsov, A. E.; Birch, K. A.; Boldyrev, A. I.; Li, X.; Zhai, H.-J.; Wang, L.-S. *Science* **2003**, *300*, 622. (b) Chen, Z.-F.; Corminboerf, C.; Heine, T.; Bohmann, J.; Schleyer, P. v. R. *J. Am. Chem. Soc.* **2003**, *125*, 13930. (c) Tanaka, H.; Neukermans, S.; Janssens, E.; Silverans, R. E.; Lievens, P. *J. Am. Chem. Soc.* **2003**, *125*, 2862. (d) Sharam, S.; Dilip, G. K.; Sourav, P. *J. Phys. Chem. A* **2004**, *108*, 628.
(8) (a) Malar, E. J. P. *J. Org. Chem.* **1992**, *57*, 3694. (b) Dransfeld, A.; Nyulászi, L.; Schleyer, P. v. R. *Inorg. Chem.* **1998**, *37*, 4413. (c) Zhai, H.-J.; Wang, L.-S.; Kuznetsov, A. E.; Boldyrev, A. I. *J. Phys. Chem. A* **2002**, *106*, 5600. (d) Kuznetsov, A. E.; Zhai, H.-J.; Wang, L.-S.; Boldyrev, A. I. *Inorg. Chem.* **2002**, *41*, 6062. (e) Ênio, D. V. B.; Willian, R. R. *Organometallics* **2004**, *23*, 5308. (f) Proft, D. F.; Fowler, P. D.; Havenith, R. W. A.; Schleyer, P. v. R.; Lier, G. V.; Geerlings, P. *Chem. Eur. J.* **2004**, *10*, 940.
(9) (a) Schleyer, P. v. R.; Kiran, B.; Simion, D. V.; Sorensen, T. S. *J. Am. Chem. Soc.* **2000**, *122*, 510. (b) Mercero, J. M.; Ugalde, J. M. *J. Am. Chem. Soc.* **2004**, *126*, 3380. (c) Mercero, J. M.; Matxain, J. M.; Ugalde, J. M. *Angew. Chem., Int. Ed.* **2004**, *43*, 5485. (d) Malar, E. J. P. *Eur. J. Inorg. Chem.* **2004**, 2723.
(10) Boldyrev, A. I.; Wang, L.-S. *J. Phys. Chem. A* **2001**, *105*, 10795.
(11) Li, X.; Zhang, H.-F.; Wang, L.-S.; Kuzenetsov, A. E.; Cannon, N. A.; Boldyrev, A. I. *Angew. Chem., Int. Ed.* **2001**, *40*, 1867.
(12) Alecandrova, A. N.; Boldyrev, A. I.; Zhai, H.-J.; Wang, L.-S.; Steiner, E.; Fowler, P. W. *J. Phys. Chem. A* **2003**, *107*, 1359.
(13) Boldyrev, A. I.; Kuznetsov, A. E. *Inorg. Chem.* **2002**, *41*, 3596.
(14) Kuznetsov, A. E.; Corbett, J. D.; Wang, L.-S.; Boldyrev, A. I. *Angew. Chem., Int. Ed.* **2001**, *40*, 3369.
(15) Chen, Z.-F.; Jiao, H.-J.; Hirschand, A.; Schleyer, P. v. R. *Angew. Chem., Int. Ed.* **2002**, *41*, 22.
(16) Zhai, H.-J.; Wang, L.-S.; Alexandrova, A. N.; Boldyrev, A. I.; Zakrzewski, V. G. *J. Phys. Chem. A* **2003**, *107*, 9319.
(17) Kuznetsov, A. E.; Boldyrev, A. I. *Struct. Chem.* **2002**, *13*, 141.
(18) King, R. B.; Heine, T.; Corminboeuf, C.; Schleyer, P. v. R. *J. Am. Chem. Soc.* **2004**, *126*, 430.
(19) Alexandrova, A. N.; Birch, K. A.; Boldyrev, A. I. *J. Am. Chem. Soc.* **2003**, *125*, 10786.
(20) Tsipis, A. C.; Tsipis, C. A. *J. Am. Chem. Soc.* **2003**, *125*, 1136.
(21) Jung, Y.; Heine, T.; Schleyer, P. v. R.; Head-Gordon, M. *J. Am. Chem. Soc.* **2004**, *126*, 3132.
(22) Li, Q. S.; Cheng, L. P. *J. Phys. Chem. A* **2003**, *107*, 2882.
(23) Aexandrova, A. N.; Boldyrev, A. I. *Inorg. Chem.* **2004**, *43*, 3588.
(24) Li, Q. S.; Jin, Q. *J. Phys. Chem. A* **2004**, *108*, 855.
(25) Li, Q. S.; Gong, L.-F. *J. Phys. Chem. A* **2004**, *108*, 4322.
(26) Schleyer, P. v. R.; Maerker, C.; Dransfeld, A.; Jiao, H.; Hommes, N. J. R. V. E. *J. Am. Chem. Soc.* **1996**, *118*, 6317.
(27) Schleyer, P. v. R.; Jiao, H.-J.; Hommes, N. J. R. v. E.; Malkin, V. G.; Malkina, O. L. *J. Am. Chem. Soc.* **1997**, *119*, 12669.
(28) Scherer, O. J.; Brück, T. *Angew. Chem., Int. Ed* **1987**, *26*, 59.
(29) (a) Baudler, M.; Akpapoglou, S. Budzikiewicz, H.; Münster, H. *Angew. Chem., Int. Ed* **1988**, *27*, 280. (b) Tracy, P. H.; Henry, F. S. *Angew. Chem., Int. Ed.* **1989**, *28*, 485.
(30) (a) Chamizo, J. A.; Mazõn, M. R.; Salcedo, R.; Tosano, R. A. *Inorg. Chem.* **1990**, *29*, 879. (b) Winter, R. F.; Geiger, W. E. *Organometallics* **1999**, *18*, 1827. (c) Cloke, F. G. N.; Green, J. C.; Hanks, J. R. Nixon, J. F.; Suter, J. L. *J. Chem. Soc., Dalton Trans.* **2000**, 3534. (d) Lein, M.; Frunzke, J.; Timoshkin, A.; Frenking, G. *Chem. Eur. J.* **2001**, *7*, 4155. (e) Frunzke, J.; Lein, M.; Frenking, G. *Organometallics* **2002**, *21*, 3351. (f) Rayó, V. M.; Frenking, G. *Chem. Eur. J.* **2002**, *8*, 4693. (g) Kudinov, A. R.; Loginov,

D. A.; Strarikova, Z. A.; Petrovskii, P. V.; Corsini, M.; Zanello, P. *Eur. J. Inorg. Chem.* **2002**, 3018.

(31) Lein, M.; Frunzke, J.; Frenking, G. *Angew. Chem., Int. Ed.* **2003**, *42*, 1303.

(32) Urnë×caius, E.; Brennessel, W. W.; Cremer, C. J.; Ellis, J. E.; Schleyer, P. v. R. *Science* **2002**, *295*, 832.

(33) Lein, M.; Frunzke, J.; Frenking, G. *Inorg. Chem.* **2003**, *42*, 2504.

(34) Frisch, M. J.; Trucks, G. W.; Schlegel, H. B.; Scuseria, G. E.; Robb, M. A.; Cheeseman, J. R.; Montgomery, Jr., J. A.; Vreven, T.; Kudin, K. N.; Burant, J. C.; Millam, J. M.; Iyengar, S. S.; Tomasi, J.; Barone, V.; Mennucci, B.; Cossi, M.; Scalmani, G.; Rega, N.; Petersson, G. A.; Nakatsuji, H.; Hada, M.; Ehara, M.; Toyota, K.; Fukuda, R.; Hasegawa, J.; Ishida, M.; Nakajima, T.; Honda, Y.; Kitao, O.; Nakai, H.; Klene, M.; Li, X.; Knox, J. E.; Hratchian, H. P.; Cross, J. B.; Bakken, V.; Adamo, C.; Jaramillo, J.; Gomperts, R.; Stratmann, R. E.; Yazyev, O.; Austin, A. J.; Cammi, R.; Pomelli, C.; Ochterski, J. W.; Ayala, P. Y.; Morokuma, K.; Voth, G. A.; Salvador, P.; Dannenberg, J. J.; Zakrzewski, V. G.; Dapprich, S.; Daniels, A. D.; Strain, M. C.; Farkas, O.; Malick, D. K.; Rabuck, A. D.; Raghavachari, K.; Foresman, J. B.; Ortiz, J. V.; Cui, Q.; Baboul, A. G.; Clifford, S.; Cioslowski, J.; Stefanov, B. B.; Liu, G.; Liashenko, A.; Piskorz, P.; Komaromi, I.; Martin, R. L.; Fox, D. J.; Keith, T.; Al-Laham, M. A.; Peng, C. Y.; Nanayakkara, A.; Challacombe, M.; Gill, P. M. W.; Johnson, B.; Chen, W.; Wong, M. W.; Gonzalez, C.; Pople, J. A. *Gaussian 03*, Revision B.03; Gaussian, Inc., Wallingford CT, 2004.

(35) Schaftenaar, G.; Noordik, J. H. *J. Comput.-Aided Mol. Des.* **2000**, *14*, 123.

(36) Because the MO's pictures computed with B3LYP/gen method are not as clear as with B3LYP/ 6-311++ G(d, p), in which the latter does not include f orbit instead of the former, meanwhile, the results are near with two different methods (see the Supporting Information), we use the MO's Pictures computed with B3LYP/gen method.

(37) Schleyer, P. v. R.; Manoharan, M.; Wang, Z. -X; Kiran, B.; Jiao, H.; Puchta, R.; Hommes, N. J. R. v. E. *Org. Lett.* **2001**, *16*, 2465.

(38) Carter, S.; Murrell, J. N. *J. Organomet. Chem.* **1980**, *192*, 399.

(39) Gomes, J. A. N. F.; Mallion, R. B. *Chem. Rev.* **2001**, *101*, 1349−1383